Journal of Alloys and Compounds 504S (2010) S443–S447

Contents lists available at ScienceDirect

Journal of Alloys and Compounds

journal homepage: www.elsevier.com/locate/jallcom

Cu/Zr nanoscaled multi-stacks fabricated by accumulative roll bonding

Y.F. Sun [a,c,*], N. Tsuji [b], H. Fujii [a], F.S. Li [c]

[a] Joining and Welding Research Institute, Osaka University, Ibaraki city, Japan
[b] Department of Materials Science and Engineering, Graduate School of Engineering, Kyoto University, Kyoto, Japan
[c] Research Centre for Materials, Department of Materials Science and Engineering, Zhengzhou University, Zhengzhou, China

ARTICLE INFO

Article history:
Received 2 July 2009
Received in revised form
23 December 2009
Accepted 8 February 2010
Available online 23 March 2010

Keywords:
Nanostructured materials
Microstructure
Mechanical properties

ABSTRACT

In this paper, six pure Cu (99.96 mass%) and five pure Zr (99.8 mass%) sheets with overall composition of $Cu_{62}Zr_{38}$ (at%) were alternatively stacked and severely deformed up to equivalent strain (ε) of 14.4 by accumulative roll bonding (ARB) technique at ambient temperature. During the ARB process, every individual Cu and Zr sheet in the multi-stacked materials decreases greatly in thickness with the increase of ε. Finally, nanolamellar structure with single layer thickness of about 20 nm can be obtained in the ARB processed Cu/Zr multi-stacks. Tensile tests were used to evaluate the mechanical properties of the ARB processed Cu/Zr multi-stacks related to the variations of ε. It reveals that the tensile strength increases greatly from 570 MPa at ε = 1.6 to 1210 MPa at ε = 14.4. However, the plastic elongation first increases from 8% at ε = 1.6 to 14% at ε = 9.6 and then decrease to 6% at ε = 14.4. The equivalent strain dominated microstructural evolution and deformation behavior of the ARB fabricated multi-stacks were put forward and discussed.

1. Introduction

Nanoscaled multilayers, which are made up of alternating layers with every individual layer of several tens of nanometer in thickness, have drawn worldwide attention in recent years due to their excellent mechanical, electrical and magnetic properties [1]. For example, nanoscaled multilayers usually exhibit high yield strength, which is close to 1/2 or 1/3 of their theoretical value at room temperature. Those containing magnetic layers are also attractive when used as magnetic recording media or microelectromechanical system [2–4]. What is more, nanoscaled multilayers consisting of two metallic layers with negative mixing enthalpy have been widely used to study the mechanism of thermally induced solid state amorphization [5–7]. However, the multilayers were usually fabricated by well-controlled layer-by-layer deposition technique such as electromagnetic sputtering [8,9], by which the total thickness of the products is limited to only a few microns due to the slow deposition rate. In such a case, nanoindentation tests were usually used to measure the multilayer hardness and elastic modulus. Although there are a few publications about the tensile testing of deposited multilayers, the tests must be carried out carefully and sometimes premature failure happens due to the existence of deposition defects [10,11]. Recently, repeatedly stacking and rolling method, or so called accumulative roll bonding (ARB) was found possible to fabricate such kind of layer-by-layer materials. By simply increasing the ARB cycles, every individual layer can be decreased to several tens of nanometer in thickness from their original millimeter-thick metal sheets [12–14]. Comparing with the deposited multilayer, the ARB processed materials contain elongated grains with large angle boundary and a great deal of dislocations due to the severe plastic deformation. In addition, ARB processed materials can be produced in bulk size and are available for the testing of global mechanical properties.

In this paper, nanoscaled multi-stacks with overall composition of $Cu_{62}Zr_{38}$ (at%) were fabricated by ARB technique after nine cycles. Note that multi-stacks were used here to be distinguished from the multilayers produced by deposition methods. The final multi-stacks are about 0.6 mm in thickness and more than 10 mm in width and length. The microstructural evolution and tensile properties of the multi-stacks with different cycles were investigated and the mechanism of the deformation behavior was put forward and discussed.

2. Experimental procedure

Pure Cu (99.96 mass%) and pure Zr (99.8 mass%) sheets with 200 mm in length and 50 mm in width were used as starting materials for the ARB process. Several Cu and Zr sheets were alternatively stacked together after degreasing and wire-brushing the sheets surfaces. Then the stacked sheets were first roll-bonded with a reduction in thickness of 75%, corresponding to an equivalent strain of 1.6. The obtained roll-bonded sheets therefore have a multi-stack structure. The obtained multi-stacks were then cut into four parts, degreased, wire-brushed, stacked, and

* Corresponding author at: Joining and Welding Research Institute, Osaka University, Ibaraki, Japan. Tel.: +81 6 68798663; fax: +81 6 68798663.
E-mail address: yfsun@jwri.osaka-u.ac.jp (Y.F. Sun).

0925-8388/$ – see front matter © 2010 Elsevier B.V. All rights reserved.
doi:10.1016/j.jallcom.2010.02.201

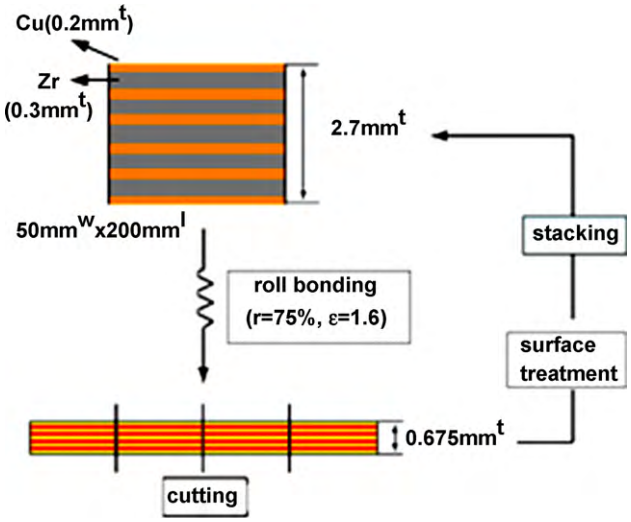

Fig. 1. Schematic illustration showing the principle of the ARB process for the Cu/Zr multi-stacks.

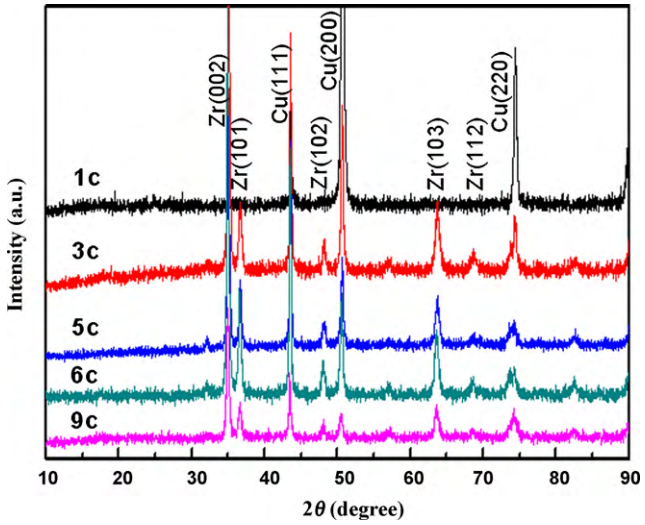

Fig. 2. XRD curves of the ARB processed Cu/Zr multi-stacks with various cycles.

then roll-bonded again as another cycle. The ARB process was repeated up to a total of nine cycles and corresponds to an equivalent strain of 14.4. All the ARB processes were carried out at room temperature. The principle of the ARB process can be known from Fig. 1. By changing the number and thickness of the pure metal sheets, multi-stacks with arbitrary overall compositions can be obtained. In the present study, six pure Cu sheets with 200 μm in thickness and five pure Zr sheet with 300 μm in thickness were used for the first cycle ARB process. Therefore, the overall composition of the multi-stacks is $Cu_{62}Zr_{38}$ (at%).

The phase constitutions of the ARB processed samples were analyzed by X-ray diffraction (XRD) and the microstructural evolutions after each ARB cycle were studied by field-emission scanning electron microscope (FE-SEM) with backscattered electron (BSE) mode and transmission electron microscopy (TEM) observation. The electron beam transparent thin foils parallel with TD were cut from the nine-cycle ARB processed sample by using focused ion beam (FIB) instrument (Hitachi FB-2000S) and were observed in a Hitachi 800 TEM at 200 kV. The ARB processed sheets were electrical discharge machined to make tensile specimen with a gauge dimension of about 5 length × 1 width × 0.6 thickness mm^3. The tensile specimen were slightly polished and the room temperature tensile tests were carried out with an Instron 4206 testing machine at a strain rate of about $1 \times 10^{-4}\ s^{-1}$. The tensile direction was parallel to the rolling direction of the ARB processed sheets.

3. Experimental results

The XRD measurements were carried out on the plane perpendicular to the transverse direction (TD) of the sheets. The typical XRD curves of the ARB processed samples with various cycles are shown in Fig. 2. From the curves, all the samples exhibit several sharp diffraction peaks, which can be indexed as Zr and Cu pure metals. The intensities of the different peaks decrease with the increase of the ARB cycles, or the refinement of the grain size. In addition, neither intermetallic compound nor phase transformation can be detected during the entire ARB process.

During the ARB process, every individual Cu and Zr layer in the multi-stacks decrease greatly in thickness due to the increase of equivalent strain. Fig. 3 shows the SEM-BSE micrographs of the Cu/Zr multi-stacks processed to various ARB cycles. The Cu and Zr layer appear in different contrast in the BSE images, namely, Cu in dark and Zr in bright. For the samples with low cycles, shear bands can be found penetrating through the entire thickness of materials. As a result, many island-like Zr blocks having diamond shapes

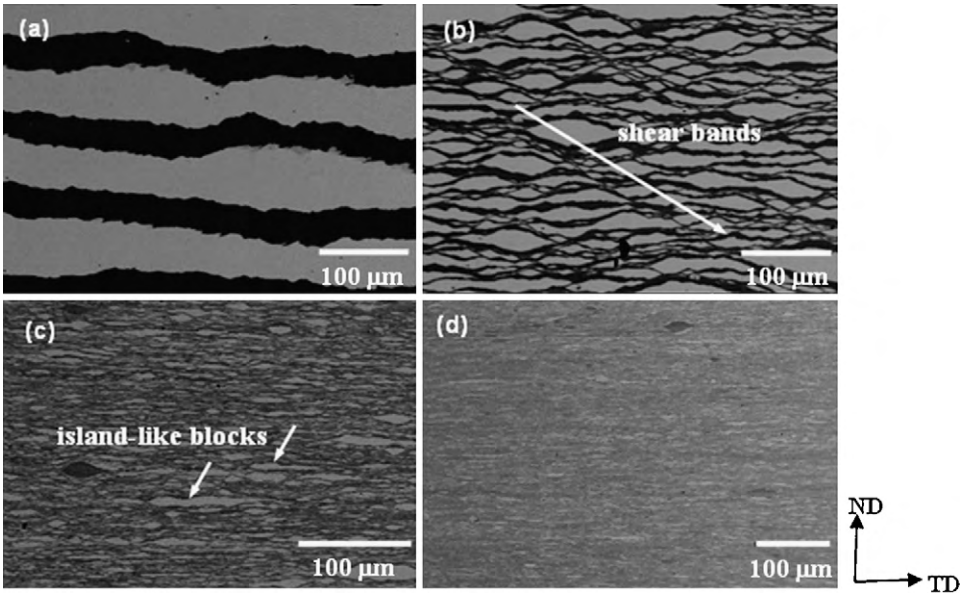

Fig. 3. SEM-BSE micrographs of the Cu/Zr multi-stacks specimens ARB processed by (a) one cycle; (b) three cycles; (c) six cycles and (d) nine cycles. Observed from TD.

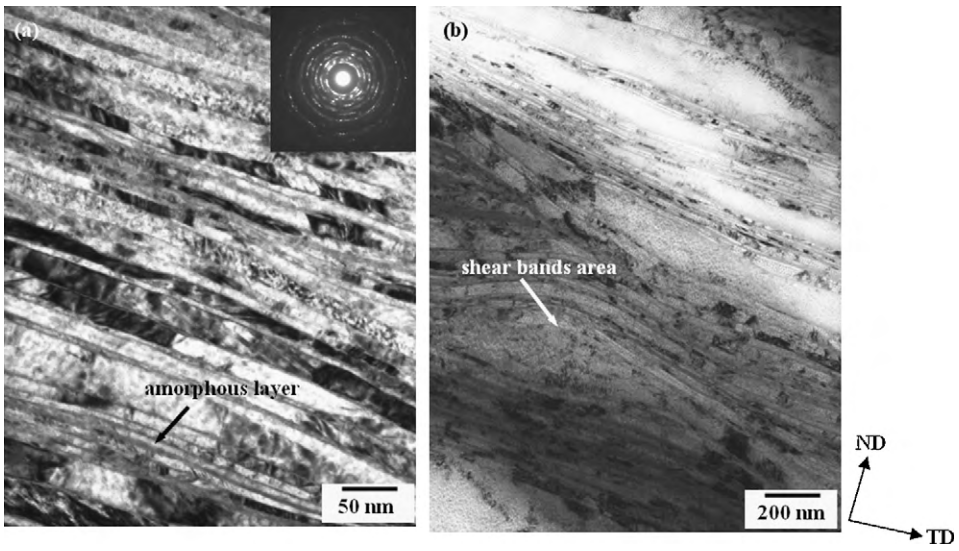

Fig. 4. TEM image showing the nanolamellar structure in the nine cycles ARB processed sample.

are formed, which are indicated by an arrow in Fig. 3(c). However, after six ARB cycles, the deformation in the multilayer becomes rather homogeneous than before. The microstructure of the sample processed after nine ARB cycles are shown in Fig. 3(d). No big island-like Zr blocks can be found and the sample exhibits greatly refined lamellar structures.

Fig. 4 shows the typical TEM image of the microstructure of the sample after nine cycles ARB process. Lamellar structure containing elongated Cu and Zr layers is visible over a large distance. The thickness of each layer was reduced from its original 0.2 mm (0.3 mm for Zr) to about 20 nm. Several very thin gray layers with no contrast inside can be found, which was indicated in Fig. 4(a) by an arrow. These gray layers are believed to have an amorphous structure due to the interdiffusion of Cu into Zr [11]. Besides the nanolamellar structure, the shear bands still can be found in the nine cycles ARB processed multi-stacks. TEM observation reveals that the microstructure in the shear bands is greatly different from that in the multi-stacks, which might be resulted from the quite large amount of plastic strain localized in the shear bands [10].

Fig. 5 shows the engineering strain–stress curves of the Cu/Zr multi-stacks processed with various ARB cycles. It reveals that the strength increases significantly with the increase of ARB cycles. All the specimens experienced a strain softening stage after yielding. The tensile strength increases from 570 MPa after one cycle ($\varepsilon = 1.6$) to 1210 MPa after nine cycles ($\varepsilon = 14.4$). However, the plastic deformation first increases from 8% after one cycle ($\varepsilon = 1.6$) to 14% after six cycles ($\varepsilon = 9.6$) and then decreases to 6% after nine cycles ($\varepsilon = 14.4$). From the appearance of the specimens after tensile tests shown in Fig. 5(b), it can be found that all the specimens fractured in a plane inclined about 45° to the tensile direction.

The fractographies of the tensile specimens are shown in Fig. 6 to reveal the fracture behavior varied with different ARB cycles. For the one-cycle ARB processed specimen shown in Fig. 6(a), the laminated stack with alternative layers can be clearly observed. Obvious crack between the neighboring layers formed along the interface, which indicated that this sample probably failed with a necking of individual layers. For the three cycles ARB processed specimen shown in Fig. 6(b), the laminate stack presents a heav-

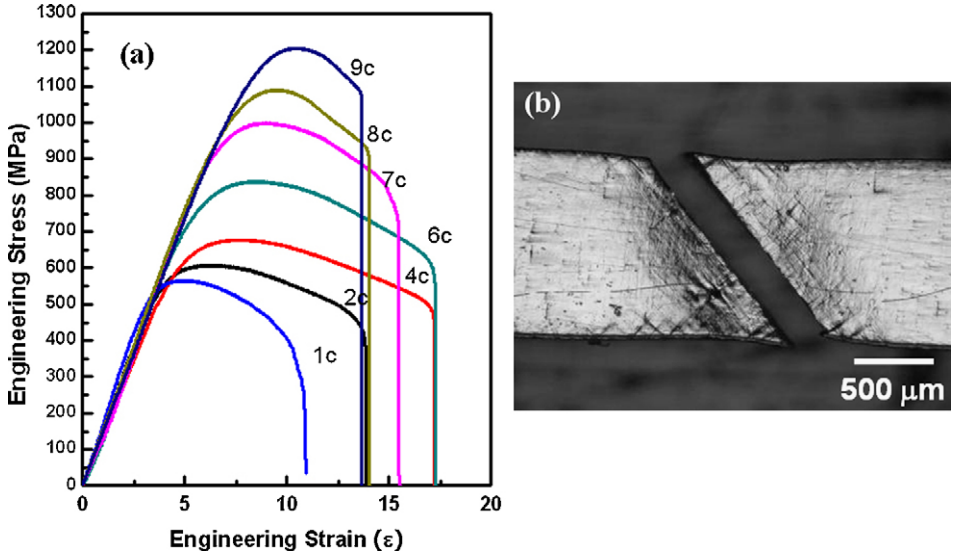

Fig. 5. (a) Tensile tests stress–strain curves of the specimens with various ARB cycles and (b) the appearance of the eight cycles ARB processed specimen after tensile tests.

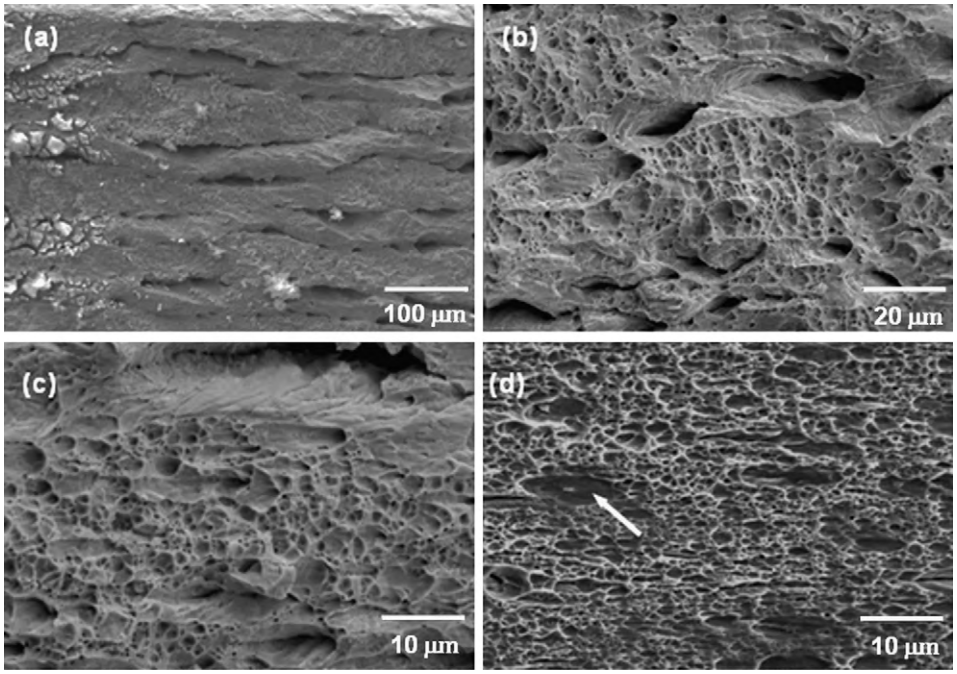

Fig. 6. SEM images showing the fractography of the Cu/Zr specimens ARB processes with (a) one cycle; (b) three cycles; (c) six cycles and (d) nine cycles.

ily dimpled and rough morphology suggesting that the specimen has been torn apart in a ductile manner. However, successive crack can still be seen at the interface between the neighboring Cu and Zr layers. For the six cycles ARB processed specimen as shown in Fig. 6(c), dimpled pattern is the dominating morphology on the fractured plane and few voids can be observed at the laminate interface. In addition, the size of the each dimple is much smaller than that observed in Fig. 6(b). For the nine cycles ARB processed specimen, only dimple patterns can be found on the fractured surface without any crack and voids. The size of dimples is smaller than that of any other dimple patterns formed on the fracture plane of other multi-stacks with less than nine cycles. However, some area with smooth surface can be found among the dimpled pattern, which is indicated by an arrow in Fig. 6(d). It was supposed that the smooth areas were formed by fracture of the shear bands area in the materials.

4. Discussion

The tensile strength of the ARB processed Cu/Zr multi-stacks increases greatly with the increase of ARB cycles due to microstructural refinement, which shows the same trend of other ARB processed materials and roughly matches the Hall–Patch relationship. After nine cycles, the strength reaches up to about 1210 MPa, a little higher than the Cu/Zr nanolaminates fabricated by sputtering deposition methods [15]. However, the tensile elongation of the Cu/Zr multi-stacks increases first and then decrease after six ARB cycles. While for the ARB processed materials consisting of commaterial layers, the tensile elongations always decrease linearly with increasing ARB cycles, regardless of the ductility of the original materials. For the Cu/Zr multi-stacks processed less than six ARB cycles, the facture topography reveals the formation of successive crack along the interface between the alternate Cu and Zr layers. It was supposed that the fracture of the multi-stacks is attributed to the inhomogeneous microstructure and the different strength between Cu and Zr. The different deformation behavior will lead to the separation of Zr and Cu layers with each other. Since the Cu is very soft and Zr is relatively hard, only Zr layer sustain the external load and will thus fracture quickly after yielding. With increasing ARB process, the difference in the mechanical properties between the two metals reduced and will definitely delays the occurrence of failure. As a result, the elongation increases correspondingly and reaches the maximum value at six ARB cycles. For the multi-stacks with more than six cycles, the strength of the alternate Cu and Zr layers become homogeneous owing to the strain-hardening effect in Cu caused by severe plastic deformation. In addition, the microstructure become rather uniform and no island-like block can be found any more. Therefore, the fracture of the multi-stacks begins to be dominated by the plastic instability, like other single-phase ultrafine grained (UFG) materials with mean grain size less than 1 μm [16].

The strain softening behavior of the ARB processed Cu/Zr multi-stacks is also different with the deposited multilayers, although they have similar nanoscaled laminated structure. From the few reports about the tensile tests of deposited multilayers, it reveals that the tensile specimen usually shows strain-hardening or perfect elastic-plastic properties, although in most cases the overall elongation is also limited within a few percent. On the contrary, it is difficult for the ARB processed multi-stacks to undergo strain-hardening stage during tensile tests, since the as-ARB processed specimens have a large amount of dislocation substructures inside the elongated grains. As a result, plastic instability usually occurs at very early stage of tensile test [16,17]. Recently it was reported that the interface between the two metals in the deposited multilayer play an important role in the mechanical properties. The coherent interface, which usually formed between metals with same crystalline structure, can result in the migration of dislocations from one layer to another. As a result, these kinds of multilayer such as Cu/Ni fcc/fcc bilayer shows higher ductility, but with lower strength. While those with incoherent interface such as Cu/Nb fcc/bcc bilayer will have high strength but low ductility, because the incoherent interface will prevents the free crossing of dislocations from the interface [18]. However, in our study, the ARB processed Cu/Ni multi-stacks also shows the similar deformation behavior with that of ARB processed Cu/Zr multi-stacks, which has an fcc/hcp incoherent interface [19].

5. Conclusion

In this paper, a series of Cu/Zr multi-stacks were prepared by ARB technique with various cycles. The microstructure and mechanical properties of the ARB processed materials were investigated and the following conclusions could be drawn.

With ARB technique, Cu/Zr multi-stacks can be fabricated by stacking pure Cu and Zr sheets. Nanoscaled structure can be obtained after nine cycles ARB process.

It reveals that the tensile strength increases greatly from 570 MPa at $\varepsilon = 1.6$ to 1210 MPa at $\varepsilon = 14.4$. However, the plastic deformation first increases from 8% at $\varepsilon = 1.6$ to 14% at $\varepsilon = 9.6$ and then decrease to 6% at $\varepsilon = 14.4$.

The fracture of the Cu/Zr multi-stacks with less than ARB six cycles is believed to be caused by the inhomogeneous microstructure throughout the sample thickness and the different strength of Cu and Zr layer. While those with more than six ARB cycles are believed to fracture due to the plastic instability and exhibit same deformation behavior with the single-phase UFG materials.

Acknowledgements

The present study was financially supported by the Grant-in-Aid for Scientific Research on Priority Area “Materials Science of Bulk Metallic Glasses” and the Global COE program “Center of Excellent for Advanced Structural and Functional Materials Design” in Osaka University both through MEXT, Japan.

References

[1] G.P. Zhang, Y. Liu, W. Wang, J. Tan, Appl. Phys. Lett. 88 (2006) 013105.
[2] A. Misra, M. Verdier, Y.C. Lu, H. Kung, T.E. Mitchell, M. Nastasi, et al., Scripta Mater. 39 (1998) 555–560.
[3] S. Matsunuma, A. Yano, E. Fujita, T. Onuma, T. Takayama, N. Ota, IEEE Trans. Magn. 38 (2002) 1622–1626.
[4] N.A. Mara, D. Bhattacharyya, P. Dickerson, Appl. Phys. Lett. 92 (2008) 231901.
[5] B.X. Liu, W.S. Lai, Z.J. Zhang, Adv. Phys. 50 (2001) 367–429.
[6] P Bhatt, S.M. Chaudhair, M. Fahlman, J. Phys. 19 (2007) 376210.
[7] R.B. Schwarz, W.L. Johnson, Phys. Rev. Lett. 51 (1983) 415–418.
[8] N. Tsuji, S. Kato, S. Ohsaki, K. Hono, Y. Minamino, J. Metastable Nanocryst. Mater. 24 (2005) 643–646.
[9] S. Ohsaki, S. Kato, N. Tsuji, T. Okubo, K. Hono, Acta Mater. 55 (2007) 2885–2895.
[10] T.G. Nieh, J. Wadsworth, Intermetallics 16 (2008) 1156–1159.
[11] T.G. Nieh, T.W. Barbee, J. Wadsworth, Scripta Mater. 41 (1999) 929–935.
[12] R.J. Hebert, J.H. Perepezko, Scripta Mater. 50 (2004) 807–812.
[13] M.C. Chen, H.C. Hsieh, W. Wu, J. Alloys Compd. 416 (2006) 169–172.
[14] Y.F. Sun, Y. Todaka, M. Umemoto, N. Tsuji, J. Mater. Sci. 43 (2008) 7457–7464.
[15] Y.M. Wang, J. Li, A.V. Hamza, T.W. Barbee, Proc. Natl. Acad. Sci. 104 (2007) 11155–11160.
[16] N. Tsuji, Y. Ito, Y. Saito, Y. Minamino, Scripta Mater. 47 (2002) 893–899.
[17] C. Kwan, Z.R. Wang, J. Mater. Sci. 43 (2008) 5045–5051.
[18] N. Loannis, Mastorakos, H.M. Zbib, D.F. Bahr, Appl. Phys. Lett. 94 (2009) 173114.
[19] Y.F. Sun, N. Tsuji, Unpublished data.